

Targeting integrins: Insights into structure and activity of cyclic RGD pentapeptide mimics containing azabicycloalkane amino acids

Laura Belvisi,^a Anna Bernardi,^a Matteo Colombo,^{a,†} Leonardo Manzoni,^b
Donatella Potenza,^a Carlo Scolastico,^{a,*} Giuseppe Giannini,^c Marcella Marcellini,^c
Teresa Riccioni,^c Massimo Castorina,^c Pietro LoGiudice^c and Claudio Pisano^{c,*}

^aDipartimento di Chimica Organica e Industriale and Centro Interdisciplinare Studi bio-molecolari e applicazioni Industriali, (CISI),
Università degli Studi di Milano, via G. Venezian 21, I-20133 Milan, Italy

^bCNR-Istituto di Scienze e Tecnologie Molecolari, via C. Golgi 19, I-20133 Milan, Italy

^cResearch and Development, Sigma-Tau, via Pontina Km 30,400, I-00040 Pomezia, Italy

Received 15 February 2005; accepted 2 August 2005

Available online 7 October 2005

Abstract—A small library of cyclic RGD pentapeptide mimics incorporating stereoisomeric 5,6- and 5,7-fused bicyclic lactams was synthesized. This library was found to contain high-affinity ligands for the $\alpha_v\beta_3$ integrin. The aim of this study was to investigate activity, selectivity, and structure of these ligands in order to identify new specific α_v -integrin antagonists that could be evaluated as tumor angiogenesis inhibitors. In vitro screening, including receptor-binding assays to purified $\alpha_v\beta_3$, $\alpha_v\beta_5$, and $\alpha_5\beta_1$ integrins, and platelet aggregation assay, revealed ST1646 as a potent, highly selective $\alpha_v\beta_3/\alpha_v\beta_5$ integrin antagonist. Structure determination of the cyclic RGD pentapeptide mimics performed by a combination of NMR spectroscopy, and molecular mechanics and dynamics calculations showed a strong dependence of the RGD cyclopeptide conformation on lactam ring size and stereochemistry. ST1646 revealed the highest ability within the library to adopt the proper RGD orientation required for binding to the $\alpha_v\beta_3$ integrin, as deduced from the recently solved crystal structure of the extracellular segment of integrin $\alpha_v\beta_3$ in complex with a cyclic pentapeptide ligand.

© 2005 Elsevier Ltd. All rights reserved.

1. Introduction

Cell adhesion is essential for the proper functionality of many physiological processes such as embryogenesis, cell differentiation, hemostasis, wound healing, and immune response, but also for pathophysiological events such as tumor cell invasion, formation of metastases, and tumor-induced angiogenesis.^{1–4} These cell adhesion processes are mediated by cell-surface receptors, among which integrins represent the most diverse and prominent class.^{5–8}

Integrins are a family of membrane-spanning adhesion receptors composed of noncovalently linked α and β sub-

units which combine to give a wide amount of heterodimers. Besides cell adhesion to extracellular matrix, integrins also mediate intracellular events that control cell shape, migration, proliferation, and survival.^{5,8} Many integrins recognize polypeptide domains containing the Arg-Gly-Asp (RGD) amino acid sequence present in several matrix associated adhesive glycoproteins.^{9,10} Specificity and efficacy of these molecular recognition processes are determined by the context of the RGD sequence, including flanking residues, conformational presentation of the triad, and individual features of the integrin binding pockets.^{11,12}

Among such RGD-dependent integrins, the vitronectin receptors $\alpha_v\beta_3$ and $\alpha_v\beta_5$ have recently received increasing attention as interesting therapeutic targets, because of their critical role in tumor-induced angiogenesis and metastasis formation.¹³

$\alpha_v\beta_3$ is not generally expressed on epithelial cells and normal endothelial cells (EC), but it is significantly upregulated on activated EC and in metastatic tumor

Keywords: Integrin receptor antagonists; Peptidomimetics; Conformational analysis; Angiogenesis inhibitors.

* Corresponding authors. Tel.: +39 02 50314090; fax: +39 02 50314072 (C.S.); tel.: +39 06 91393760; fax: +39 06 91393988 (C.P.); e-mail addresses: carlo.scolastico@unimi.it; claudio.pisano@sigma-tau.it

† Present address: Nikem Research, via Zambelletti 25, I-20021, Baranzate di Bollate (MI), Italy.

cells. Growth factors such as fibroblast growth factor-2 (FGF2) and tumor necrosis factor- α (TNF α) stimulate $\alpha_v\beta_3$ expression in the developing chick chorioallantoic membrane (CAM) and in the angiogenesis model of the rabbit cornea.¹⁴ The importance of $\alpha_v\beta_3$ in tumor angiogenesis is also demonstrated by the fact that $\alpha_v\beta_3$ antagonists, including cyclic RGD peptides and monoclonal antibodies, were successfully used to inhibit blood vessel development and tumor growth in different models.^{15,16} It is noteworthy that $\alpha_v\beta_3$ antagonists have very little effect on pre-existing blood vessels, indicating the usefulness of targeting this receptor for therapeutic benefit without adverse side effects.

Recent studies have implicated a related integrin, $\alpha_v\beta_5$, in angiogenesis, possibly via a signaling pathway distinct from that of $\alpha_v\beta_3$ and activated by a different growth factor.¹⁷ The existence of distinct angiogenic pathways can be explained with the prevalence of specific growth factors and/or cell-adhesive proteins in different conditions.

Furthermore, many steps that characterize the acquisition of invasive and metastatic potential by tumor cells, such as intravasation, adhesion to the vessel wall, extravasation, infiltration, and proliferation into target tissue, involve integrins. This implies that migratory tumor cells express the integrin receptors and the enzymatic machinery for recognition, adhesion, matrix degradation, and penetration involved in cell–cell and cell–ECM interactions. For example, integrin $\alpha_v\beta_3$ expression is upregulated on certain invasive tumors including metastatic melanoma¹⁸ and late stage glioblastoma.¹⁹ Thus, inhibition of $\alpha_v\beta_3$ receptor, in addition to blocking tumor-induced angiogenesis, has impact on a number of mechanisms involved in tumor progression.

Taken together, these results suggest that selective $\alpha_v\beta_3$ and/or $\alpha_v\beta_5$ antagonists may represent a promising approach for the inhibition of tumor angiogenesis and tumor growth. Various RGD-containing cyclic peptides have been developed by different groups as active and selective integrin antagonists that compete with matrix molecules for specific integrin receptors.^{20–22}

An efficient procedure of spatial screening, performed by Kessler et al. and based on the synthesis of stereoisomeric cyclic peptide libraries, led to the highly active $\alpha_v\beta_3$ -selective first-generation cyclic pentapeptide cyclo(Arg-Gly-Asp-D-Phe-Val).^{23–25} Extensive modifications of this lead structure with different peptidomimetics and carbohydrate scaffolds have been performed, and new potent antagonists have been identified.^{26–28} The systematic derivatization of the lead peptide resulted in the N-alkylated cyclopeptide cyclo(Arg-Gly-Asp-D-Phe-[NMe]Val),²⁹ which has entered clinical phase II studies as anticancer drug (cilengitide, EMD121974).

Recently, our group has reported a library of cyclic RGD pentapeptide mimics, based on azabicycloalkane amino acid scaffolds of type I (Fig. 1).³⁰ Stereoisomeric 5,6- and 5,7-fused bicyclic lactams showing different reverse-turn mimetic properties^{31–33} were exploited as

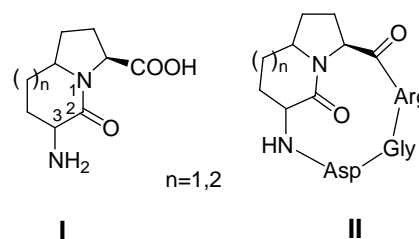


Figure 1. Azabicycloalkane scaffolds of type I and general formula II of the library cyclo(Arg-Gly-Asp-Lactam).

dipeptide analogs for the synthesis of a library of general formula cyclo(Arg-Gly-Asp-Lactam) II (Fig. 1). This library was found to contain specific high-affinity ligands

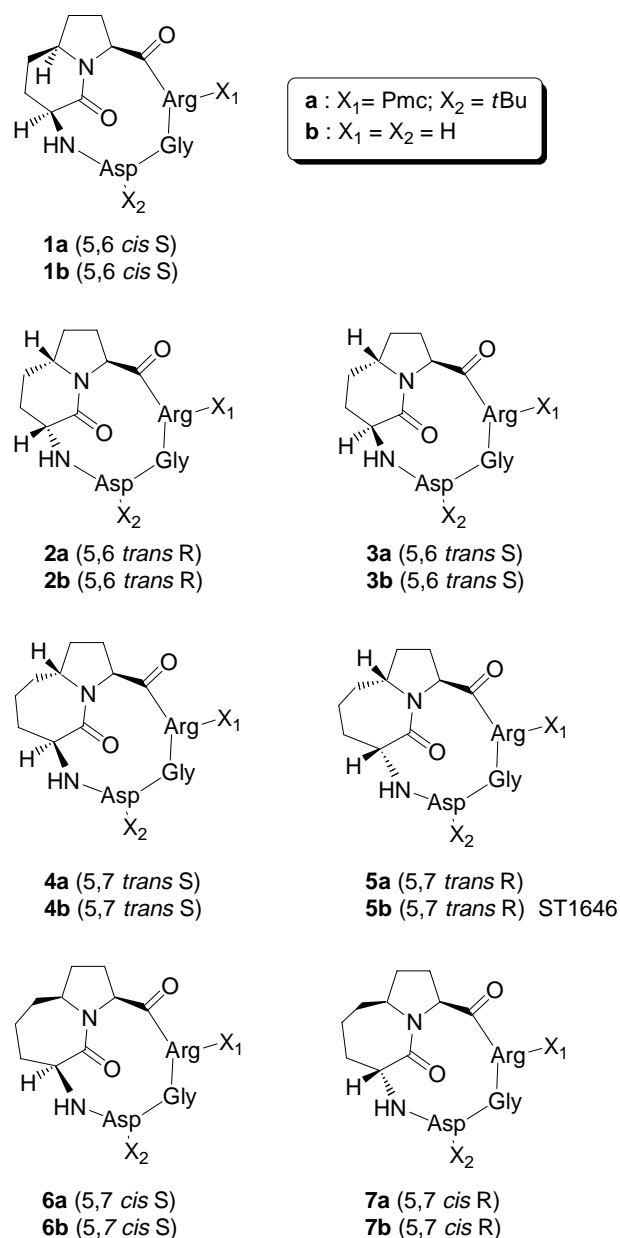


Figure 2. Cyclic RGD pentapeptide mimics cyclo(Arg-Gly-Asp-Lactam) 1–7. The ring size and the stereochemistry at the bridgehead (*cis* or *trans*) and at the C3 (*S* or *R*) carbon of the bicyclic lactam are reported in parentheses.

of $\alpha_v\beta_3$ integrin, that are presently being evaluated as very promising antiangiogenic drugs. Among the peptides tested, compound ST1646 (Fig. 2 and Table 1, compound **5b**) showed the highest affinity to $\alpha_v\beta_3$, inhibiting echistatin binding to $\alpha_v\beta_3$ with an IC_{50} of 3.8 ± 0.9 nM.

Herein, we report the in vitro screening of activity and selectivity, and the structure determination by spectroscopic and computational means of the small library of cyclic RGD pentapeptide mimics cyclo(Arg-Gly-Asp-Lactam). Effects of the structural constraint introduced by the bicyclic template on the conformation of the RGD sequence have been especially investigated by examining the dependence of the cyclopeptide conformation on lactam ring size and stereochemistry. Moreover, efforts to evaluate the ability of the library members to adopt the proper RGD orientation required for binding to the $\alpha_v\beta_3$ integrin have been carried out, using the recently solved crystal structure of the cyclic pentapeptide ligand EMD121974 in complex with the extracellular segment of $\alpha_v\beta_3$ integrin.³⁴

2. Results

2.1. Screening in the solid-phase receptor-binding assay

The small library of seven cyclic RGD pentapeptide mimics incorporating stereoisomeric 5,6- and 5,7-fused bicyclic lactams was screened in vitro for activity and selectivity. The replacement of the D-Phe-Val or the D-Phe-[NMe]Val dipeptide present in the lead structures

Table 1. In vitro binding of RGD peptides to purified integrin receptors^a

Compound	$IC_{50} \pm SD$ (nM)		
	^[125I] Echistatin binding to $\alpha_v\beta_3$	^[125I] Echistatin binding to $\alpha_v\beta_5$	^[125I] Fibrinogen binding to $\alpha_5\beta_1$
Echistatin	0.29 ± 0.08	0.29 ± 0.02	
c(RGDfV)	196 ± 17	0.11 ± 0.03	
EMD121974	18.9 ± 3.1	0.13 ± 0.01	>10,000
Vitronectin	44 ± 17	11.8 ± 2.7	
Fibronectin	835 ± 287	162 ± 45	
Fibrinogen	17408 ± 2966		
1b	154 ± 21	>1000	
2b	14.3 ± 4.7	9.02 ± 1.9	
3b	202 ± 23	>1000	
4b	461 ± 122	1.3 ± 0.4	
5b (ST1646)	3.8 ± 0.9	1.39 ± 0.2	>10,000
6b	491 ± 131	>1000	
7b	3343 ± 230	>1000	

^a The compounds were tested in a solid-phase receptor assay for their ability to compete for the binding of [^{125I}]echistatin to either purified $\alpha_v\beta_3$ or $\alpha_v\beta_5$ and for the binding of [^{125I}]fibrinogen to purified $\alpha_5\beta_1$. Integrin-coated 96-well plates were incubated with radiolabeled ligand in the presence of serially diluted competing compounds. After incubation, plates were washed and radioactivity was measured with a γ -counter. The IC_{50} was calculated as the concentration of compound required for 50% inhibition of ligand binding as estimated by the Allfit program. Values are means \pm standard deviation of the determinations from three or four independent experiments.

c(RGDfV)^{23–25} or EMD121974,²⁹ respectively, with aza-bicycloalkane scaffolds showing different reverse-turn mimetic properties could constrain the RGD sequence into different conformations and possibly provide the required activity and selectivity for integrin antagonism. To test this hypothesis the compounds were screened in a solid-phase assay for their ability to compete with radiolabeled echistatin for the binding to purified human $\alpha_v\beta_3$ and $\alpha_v\beta_5$ and to compete with radiolabeled fibrinogen for the binding to $\alpha_5\beta_1$ integrin. The well-characterized integrin antagonists cyclic pentapeptides c(RGDfV) and EMD121974, as well as the natural integrin ligands vitronectin, fibronectin, and fibrinogen, were used as positive controls (Table 1).

Among the seven peptides tested, compounds **2b** and **5b** showed the highest affinities to $\alpha_v\beta_3$, and inhibited radiolabeled echistatin binding to $\alpha_v\beta_3$ with an IC_{50} of 14.3 ± 4.7 and 3.8 ± 0.9 nM, respectively. Interestingly, the affinity of **5b** for the $\alpha_v\beta_3$ integrin in this kind of assay was almost 50 and 5 times higher than the affinity of the lead structures c(RGDfV) and EMD121974, used as reference compounds.

The most active compound **5b** (ST1646) inhibited radiolabeled echistatin binding to $\alpha_v\beta_5$ with IC_{50} equal to 1.4 ± 0.2 nM. Like echistatin, compounds **2b** and **5b** have similar potency against $\alpha_v\beta_3$ and $\alpha_v\beta_5$ whereas c(RGDfV) and EMD121974 are, respectively, over 1000- and 100-fold more selective for $\alpha_v\beta_5$ in this kind of assay (Table 1).³⁵

Selectivity of compound **5b** was demonstrated by its inability to compete with radiolabeled fibrinogen for $\alpha_5\beta_1$ interaction ($IC_{50} > 10^{-5}$ M). Similar to c(RGDfV), ST1646 was 500 times less active than echistatin in preventing in vitro platelet aggregation in response to thrombin receptor-activating peptide (Table 2). Thus, the inability of ST1646 to inhibit $\alpha_{11b}\beta_3$ -mediated platelet aggregation confirmed the selectivity of this compound.

Table 2. Effect of RGD peptides on TRAP-induced guinea pig platelet aggregation^a

Compound	$IC_{50} \pm SD$ (μ M)
Echistatin	0.018 ± 0.0001
c(RGDfV)	10.5 ± 1.7
EMD121974	>10
2b	>10
5b (ST1646)	12 ± 2.2

^a Peptide-mediated inhibition of platelet aggregation was determined by incubating platelet-rich plasma (PRP) with different concentrations of the peptides or with vehicle and quantifying the extent of platelet aggregation by a turbidimetric method within 4 min after the addition of the agonist 11-mer thrombin receptor activating peptide (TRAP). The results are plotted (Allfit program) and expressed as the antagonist concentration that inhibited 50% of platelet aggregation. Values are means \pm standard deviation of the determinations from three or four independent experiments. As shown, ST1646 was 500-fold less active than echistatin in preventing in vitro platelet aggregation, demonstrating a low affinity for the $\alpha_{11b}\beta_3$ receptor.

Table 3. Effect of RGD peptides on BMEC adhesion to vitronectin and fibronectin^a

Compound	IC ₅₀ ± SD (μM)	
	EC adhesion to vitronectin	EC adhesion to fibronectin
c(RGDfV)	10.3 ± 2.6	>100
EMD121974	2.7 ± 0.3	66.8 ± 14
1b	>100	>100
2b	53.1 ± 6.1	53.9 ± 13.9
3b	>100	>100
4b	43.2 ± 5.6	—
5b (ST1646)	0.9 ± 0.2	37.5 ± 2.6
6b	>100	>100
7b	>100	>100

^a Bovine microvascular endothelial cell (BMEC) adhesion was performed allowing the cells to adhere to 96-well plates coated with either fibronectin or vitronectin for 1–3 h at 37 °C, in the presence or absence of various concentrations of RGD peptides. Toluidine-stained adherent cells were quantified on a microtiter plate reader at 600 nm. Results, expressed as mean compound concentration ± SD that inhibited 50% of cell adhesion (from three independent experiments), show that ST1646 was the most active among the compounds tested.

2.2. Inhibition of cellular adhesion to vitronectin and fibronectin

To assess the ability of the cyclic RGD pentapeptide mimics to behave as integrin antagonists for ECs, BMECs were allowed to adhere to immobilized vitronectin or fibronectin in the presence of increasing concentrations of the synthetic pseudopeptides (ranging between 0.1 and 100 μM). As shown in Table 3, compound **5b** (ST1646) significantly inhibited cell adhesion

to either vitronectin or fibronectin in a dose-dependent manner with IC₅₀ values equal to 0.9 and 37.5 μM, respectively. For both cell-adhesion proteins, the activity of this compound was higher, on a molar basis, than those of c(RGDfV) and of EMD121974. In contrast, all the other RGD-containing cyclic pseudopeptides did not exert a significant antagonist activity. Similar results were obtained when the compounds were tested on human microvascular endothelial cells (data not shown).

Taken together, the in vitro screening results indicate that **5b** (ST1646) represents a potent and selective α_vβ₃/α_vβ₅ integrin antagonist to be tested for anti-angiogenic activity in vivo. To this aim, a multigram scale synthesis of **5b** was developed by optimizing both the bicyclic lactam preparation and the peptide synthesis.³⁶

2.3. Computational studies

Monte Carlo/energy minimization (MC/EM) conformational searches designed to investigate the effects of the bicyclic lactam on the cyclopeptide conformation were performed on the cyclo(Ala-Gly-Ala-Lactam) pentapeptide analogs **1c–7c** (Table 4). The principal types of backbone geometries calculated for these compounds and their relative stabilities are given in Table 4. The minimum energy conformations of these cyclic pentapeptide mimics are characterized by the formation of peptide secondary structures, in particular γ- and β-turns, that may be stabilized by intramolecular hydrogen bonds. In γ-turns, the C=O of the first residue (*i*) may be hydrogen bonded to the NH of the third residue (*i* + 2), giving rise to a seven-membered ring. In β-turns, the C=O of the first residue (*i*) may be hydrogen bonded

Table 4. Characteristics of low-energy conformers (MC/EM, AMBER*, and H₂O GB/SA) calculated for cyclic pentapeptide mimics **1c–7c** cyclo(Ala-Gly-Ala-Lactam)^a

Compound (no. of conf. <3 kcal/mol)	ΔE (kcal/mol)	Conformation	CβArg–CβAsp distance (Å)
1c cyclo(Ala-Gly-Ala-5,6 <i>cis</i> S) (6 conformers)	0.0	Type SII—γ(Gly)/βII'(Gly-Asp) ^b	8.1
	2.4	Type SIII—Inv.γ(Asp)/βII'(Gly-Asp) ^b	8.6
	2.9	Type SI—βII'(lactam)/γ(Gly)	7.4
2c cyclo(Ala-Gly-Ala-5,6 <i>trans</i> R) (3 conformers)	0.0	Type SIV—βI(Pro-Arg)/Inv.γ(Asp)	9.4
	0.8	Type SIII—Inv.γ(Asp)/βII'(Gly-Asp) ^b	8.6
3c cyclo(Ala-Gly-Ala-5,6 <i>trans</i> S) (4 conformers)	0.0	Type SI—βII'(lactam)/γ(Gly)	7.7
	0.5	Type SIV—βI(Pro-Arg) ^c /Inv.γ(Asp)	9.4
	0.6	Type SII—γ(Gly)/βII'(Gly-Asp) ^b	8.2
	0.9	Type SIII—Inv.γ(Asp)/βII'(Gly-Asp) ^b	8.8
4c cyclo(Ala-Gly-Ala-5,7 <i>trans</i> S) (10 conformers)	0.0	Type SII—γ(Gly)/βII'(Gly-Asp) ^b	8.3
	0.4	Type SIII—Inv.γ(Asp)/βII'(Gly-Asp) ^b	8.7
	0.9	Type SIV—βI(Pro-Arg) ^c /Inv.γ(Asp)	9.4
	1.4	Type SI—βII'(lactam)/γ(Gly)	7.7
5c cyclo(Ala-Gly-Ala-5,7 <i>trans</i> R) (5 conformers)	0.0	Type SIII—Inv.γ(Asp)/βII'(Gly-Asp) ^b	8.5
	0.2	Type SII—γ(Gly)/βII'(Gly-Asp) ^b	8.2
	1.0	Type SIV—βI(Pro-Arg)/Inv.γ(Asp)	9.3
6c cyclo(Ala-Gly-Ala-5,7 <i>cis</i> S) (3 conformers)	0.0	Type SIV—βI(Pro-Arg)/Inv.γ(Asp)	9.4
	0.1	Type SIII—Inv.γ(Asp)/βII'(Gly-Asp) ^b	8.7
7c cyclo(Ala-Gly-Ala-5,7 <i>cis</i> R) (5 conformers)	0.0	Type SIII—Inv.γ(Asp)/βII'(Gly-Asp) ^b	8.6
	0.7	Type SIV—βI(Pro-Arg)/Inv.γ(Asp)	9.3

^a The lowest energy conformer of each conformational family within 3 kcal/mol of the global minimum is described.

^b Distorted type II' β-turn.

^c Distorted type I β-turn.

to the NH of the fourth residue ($i + 3$), forming a ten-membered ring. The classification into specific β -turn or γ -turn structural types was based on the geometry of the peptide backbone, as described by the ϕ and ψ torsion angles in residues $i + 1$ and $i + 2$ (β -turn) or in residue $i + 1$ (γ -turn). Accordingly, assignment of a low-energy conformation to a particular turn type was made, where possible, on the basis of the ideal ϕ and ψ torsion angles ($\pm 30^\circ$) reported by Rose et al.³⁷

The structural constraints introduced by the cyclic pentapeptide system and the azabicycloalkane amino acid force the compounds to assume only few conformations. As shown in Table 4, four significant geometries (denoted as SI, SII, SIII, and SIV) can be detected among the conformers within 3 kcal/mol of the global minimum calculated for compounds **1c–7c** in water, as implicitly represented by the GB/SA solvation model.⁴⁷ Each cyclopeptide geometry shows a specific β/γ -turn arrangement that induces a differently kinked conformation of the AGA sequence with a characteristic C β (Ala)–C β (Ala) distance value. The strongest kink and the shortest C β –C β distances can be observed in SI structural type, featuring a β II'/ γ -turn arrangement with the bicyclic template in the $i + 1$ and $i + 2$ positions of the β II'-turn and the Gly residue in the $i + 1$ position of the γ -turn. On the opposite

site, the most extended conformation of the AGA sequence and the highest C β (Ala)–C β (Ala) distance values can be observed in SIV geometry, featuring a β I-turn/inverse γ -turn arrangement with the Pro residue of the lactam in the $i + 1$ position of the β I-turn and the Ala replacing the Asp residue in the $i + 1$ position of the inverse γ -turn. Intermediate situations in terms of kink and distance are introduced by the SII and SIII structural types, featuring a γ -turn at Gly or an inverse γ -turn at Ala (Asp), respectively, and a common distorted β II'-turn with Gly at the $i + 1$ position. As an example, the conformers calculated for compound **3c** are reported in Figure 3 to show the four cyclopeptide conformations. Moreover, a strong dependence of the preferred cyclopeptide conformations on lactam ring size and stereochemistry can be observed in Table 4. For instance, the SI structural type can be detected only among the conformers of cyclopentapeptides incorporating β -turn inducer bicyclic lactams, like **1c**, **3c**, and **4c**, with a relative stability that increases as the turn mimetic properties of the scaffold improve.³⁸

MC/SD simulations of the cyclic RGD pentapeptide mimics **1b–7b** were then performed at 300 K, starting from the cyclopeptide backbone geometries located by the previous MC/EM step. For each compound, conver-

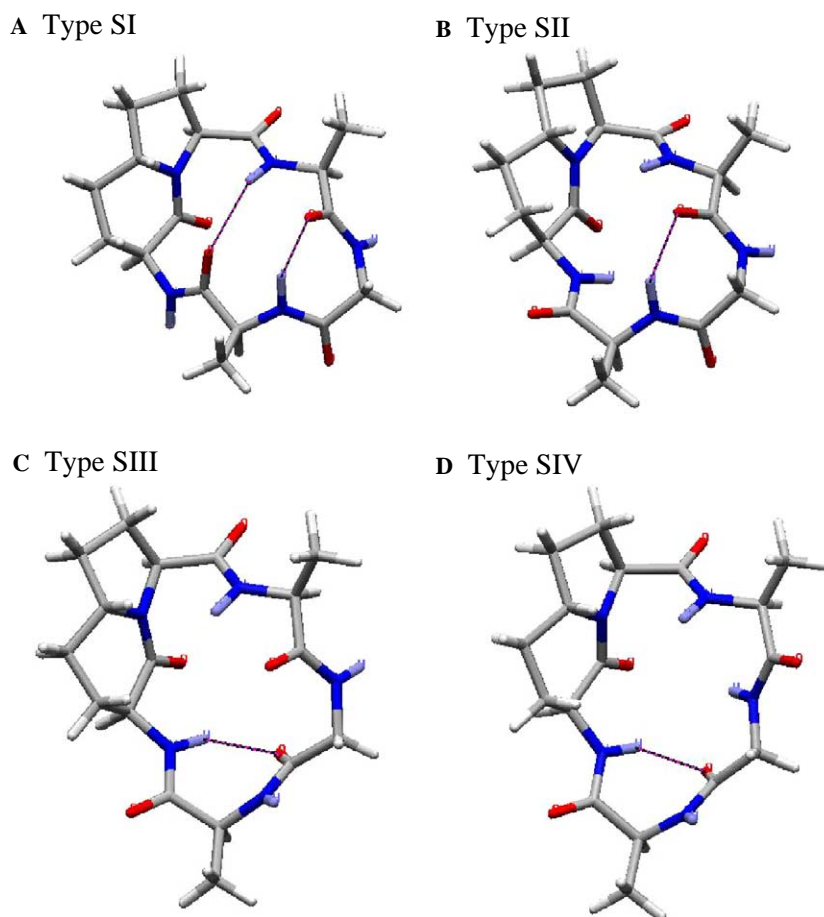


Figure 3. Minimum energy conformations of compound **3c** cyclo(Ala-Gly-Ala-5,6 *trans* S). (A) Type SI, β II'(lactam)/ γ (Gly). (B) Type SII, γ (Gly)/distorted β II'(Gly-Asp). (C) Type SIII, inverse γ (Asp)/distorted β II'(Gly-Asp). (D) Type SIV, β I(Pro-Arg)/inverse γ (Asp). The formation of hydrogen bonds in which HO distance < 2.5 Å, N–HO bond angle > 120°, and HO=C angle > 90° is indicated by a violet line.

Table 5. Population of H-bonds during the 10 ns MC/SD simulations (AMBER*, H₂O GB/SA) of cyclic RGD pentapeptide mimics **1b–7b** cyclo(Arg-Gly-Asp-Lactam)

Donor	Acceptor	Turn	% H-bond ^a						
			1b	2b	3b	4b	5b	6b	7b
Asp NH	Arg CO	γ(Gly)	31	3	45	24	11	3	5
Lact. NH	Gly CO	Inv. γ(Asp)	23	40	16	23	33	57	32
Lact. NH	Arg CO	βII'(Gly-Asp)	9 + 47 ^b	0 + 20 ^b	1 + 14 ^b	6 + 48 ^b	0 + 50 ^b	0 + 28 ^b	0 + 42 ^b
Arg NH	Asp CO	βII'(lactam)	16 + 7 ^b	0 + 1 ^b	20 + 44 ^b	9 + 15 ^b	0 + 2 ^b	0 + 2 ^b	0 + 0 ^b
Gly NH	Lact. CO	βI(Pro-Arg)	6 + 21 ^b	26 + 34 ^b	5 + 26 ^b	5 + 18 ^b	1 + 12 ^b	13 + 55 ^b	4 + 15 ^b

^a % H-bond is the percentage of conformations sampled during the simulation in which HO distance < 2.5 Å

^b Percentage of conformations featuring a distorted β-turn in which 2.5 Å < HO distance < 4 Å.

gence of the simulations was obtained and a nice agreement with the results provided by the MC/EM searches was observed, in terms of backbone geometries, intramolecular H-bonds, and Cβ–Cβ distances. Population of H-bonds during the 10 ns MC/SD simulations in GB/SA water of **1b–7b** is reported in Table 5. According to the corresponding Arg-NH...O=C-Asp H-bond, the βII'-turn at bicyclic lactam is significantly populated only during the MC/SD simulations of **1b**, **3b**, and **4b**.

2.4. NMR spectroscopy

The conformational behavior of protected RGD-pentapeptides **1a–5a** was elucidated by their ¹H NMR features in CDCl₃ solution. The intrinsic folding propensity of peptides is determined by several factors, including hydrogen-bond-driven processes. So, we undertook a conformational study of protected RGD-pentapeptides **1a–5a**, in a relatively nonpolar solvent

(chloroform), which does not offer strong hydrogen bond competition.

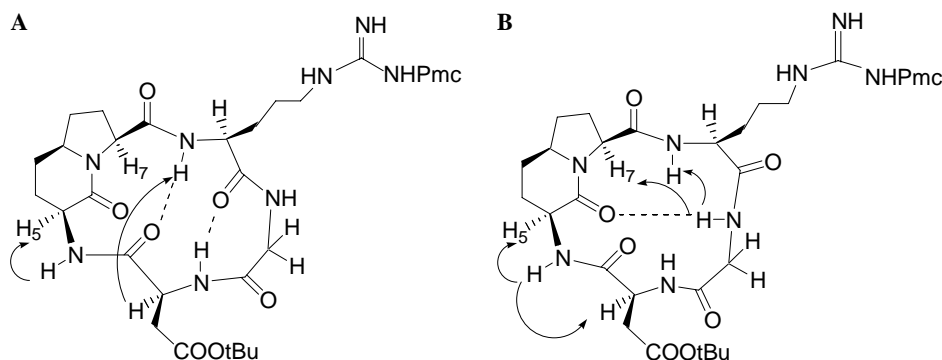
We first performed ¹H NMR analysis to determine the lowest concentration at which aggregation was not significant. Then, the internal hydrogen-bonding equilibria in these compounds were evaluated by measuring the chemical shift of the N–H protons and their temperature coefficients (Δδ/ΔT). NOESY spectra were recorded to investigate both sequential and long-range nOe's that provide evidences of preferred conformations and give insight into stable reverse turn conformations.

In the ¹H NMR spectrum of compound **1a** (5,6 *cis* 3S) the chemical shifts of amide protons Arg-NH, Gly-NH, and Asp-NH (Table 6)³⁹ suggest that they are all involved in a hydrogen bond interaction, but each to a different extent. The temperature dependence (ΔδNH/ΔT) (Table 6) also reflects this behavior and suggests that the participation of the hydrogen bond of Arg-

Table 6. Chemical shifts and temperature coefficients of NH protons of compounds **1a–5a** in CDCl₃^a

NH	1a (5,6 <i>cis</i> S)		2a (5,6 <i>trans</i> R)		3a (5,6 <i>trans</i> S)		4a (5,7 <i>trans</i> S)		5a (5,7 <i>trans</i> R)	
	¹ H δ (ppm)	ΔδNH/ΔT (ppb/K)	¹ H δ (ppm)	ΔδNH/ΔT (ppb/K)	¹ H δ (ppm)	ΔδNH/ΔT (ppb/K)	¹ H δ (ppm)	ΔδNH/ΔT (ppb/K)	¹ H δ (ppm)	ΔδNH/ΔT (ppb/K)
Arg	7.80	-5.6	7.18	-0.5	7.06	-1.6	7.19	-3.0	6.99	-12.0
Gly	8.83	-6.5	7.93	-2.0	8.06	-12.8	7.78	-8.0	7.61	-4.2
Asp	7.62	-0.8	7.56	-8.0	7.02	-9.5	7.94	-12.0	7.62	-12.0
Lactam	6.79	+1.8	7.35	-0.7	7.59	-5.7	7.64	-6.0	7.49	-1.2

^a The temperature coefficients for 5,6 bicyclic derivatives were obtained in the temperature range (250–300 K); for the 5,7 bicyclic derivatives the range was 290–320 K.

**Figure 4.** Significant contacts NOE and β- and γ-turn conformations preferred by compound **1a**. These conformations are not exclusive and can occur simultaneously; for simplicity we depicted them separately. The dotted lines indicate hydrogen bonds.

NH and Gly-NH in **1a** becomes much more significant in the low temperature region. At the same time, the positive value of $\Delta\delta\text{NH}/\Delta T$ (+1.8 ppb/K, 6.79 ppm) for Lactam-NH indicates that at low temperature, also the small amount of hydrogen bond experienced by Lactam-NH was broken.

The NOE patterns and the spin–spin coupling $^3J_{\text{HNH}_\alpha}$ expected for a β -turn conformation are observed in compound **1a**. In fact, the long range NOEs of Gly-NH with Arg-NH and H7 and the extreme value of 3J (ArgNH-H8 = 9 Hz) are indicative of a β -turn conformation (Fig. 4B). This β -turn was stabilized by a hydrogen bond between Gly-NH and C=O of the bicyclic lactam. Moreover, Arg-NH forms an additional hydrogen bond with C=O of Asp, stabilizing a β -turn with the proline residue at the $i + 2$ position (Fig. 4A). The long range NOE between Arg-NH and Asp-H α confirms this conformation.

At the same time, the presence of a γ -turn (Fig. 4A), observed by modeling, was confirmed by the temperature dependence and the value of chemical shift of the amide proton Asp-NH. The contact NOE between Lactam-NH and H5 suggests a conformation where Lactam-NH is not involved in an internal hydrogen bond. An indication of the rigidity of this part of the cycle comes from the observation that the side-chain protons of the Asp residue have restricted rotation: the chemical shifts for the two β protons are very different (0.5 ppm). In Figures 4A and B, the significant contacts NOE, and β - and γ -turn conformations preferred by compound **1a** are reported. These conformations are not exclusive and can occur simultaneously; for simplicity, we depicted them separately. Thus, in CDCl₃ solution, the pseudopeptide **1a** assumes a very compact folding stabilized by three hydrogen bonds.

The peptidomimetic **2a** is more prone to aggregation so the spectra were performed below 2 mM CDCl₃ solution. In this compound, the configuration of the scaffold (5,6 *trans* *R*) arranges the peptidic cycle so that the Arg residue is found above the plane of the bicyclic lactam,

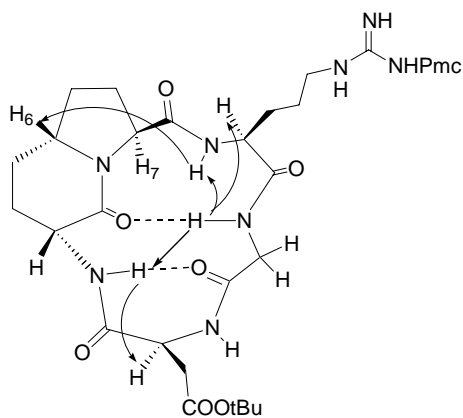


Figure 5. Significant contacts NOE and conformation preferred by compound **2a**. Pseudopeptide **2a** can fold into a β -hairpin-like conformation where the β -turn is stabilized by a second hydrogen bond to form (10 + 14) hydrogen bonded rings.

while the Lactam-NH bond is oriented below the plane. Hence, the Arg-NH cannot form a 10-membered ring hydrogen bond (β -turn) with C=O Asp (below the medium plane) but, if any, a γ -turn with lactamic C=O. In fact, Arg-NH exhibits a medium NOE cross-peak with H6 (Fig. 5). The chemical shifts and the temperature dependence of amide protons Gly-NH and Lactam-NH (respectively, 7.93 ppm and -2 ppb/K for Gly-NH; 7.35 ppm and -0.7 ppb/K for Lactam-NH) (Table 6) are typical of protons locked in a hydrogen bond. NOESY spectra of compound **2a** show NOEs between Gly-NH and Arg-NH, and between Gly-NH and Arg-H α (Fig. 5). These are indicative of a β -turn conformation stabilized by a hydrogen bond between Gly-NH and lactamic C=O. Moreover, Gly-NH shows a NOE cross-peak with Lactam-NH as well as the amidic proton Lactam-NH that is inside to the cyclic pentapeptide and can experience a hydrogen bond with C=O of Gly. These data indicate that **2a** can fold into a β -hairpin-like conformation where the β -turn is stabilized by a second hydrogen bond (Fig. 5).

The ¹H NMR spectrum of compound **3a** (5,6 *trans* *S*) shows broad signals, also in the CH α region, indicative of a slow equilibrium between more equivalent conformations. In fact, the spectra of the same compound recorded at different temperature (CDCl₃, 330 K) or in DMSO solution show sharp signals. The 5,6 *trans* 3*S*-fused bicyclic lactam used as external constraints for the RGD tripeptide in the mimic **3a** is a very good inductor of β -turn.³² Indeed, the chemical shift of amidic Arg-NH of compound **3a** was at 7.06 ppm ($\Delta\delta\text{NH}/\Delta T = -1.6$ ppb/K) and it represents the behavior of an amide proton in the hydrogen-bonded state. But, the temperature dependence ($\Delta\delta\text{NH}/\Delta T$) and the chemical shift value (Table 6) of amide proton Lactam-NH hint toward involvement in a hydrogen bond. Most likely, Lactam-NH is inside to the cyclopeptide and, in agreement with modeling, experiences a seven-membered hydrogen-bonded ring with C=O of Gly. The formation of this γ -turn is exclusive with the presence of β -turn where Arg-NH experiences a hydrogen bond. Compilation of NOE data (Fig. 6) and NH chemical shift temperature dependence for protons Gly-NH and Asp-NH (respectively, -12.8 and -9.5 ppb/K) in compound **3a** provide further evidence for multiple folded conformations in equilibrium. So, the NMR data obtained for **3a** do not give evidence of a unique solution conformation.

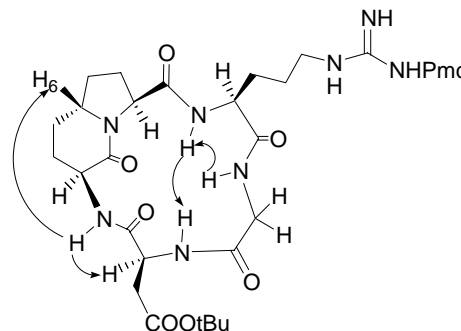


Figure 6. Key NOE connectivities found for mimetic **3a**.

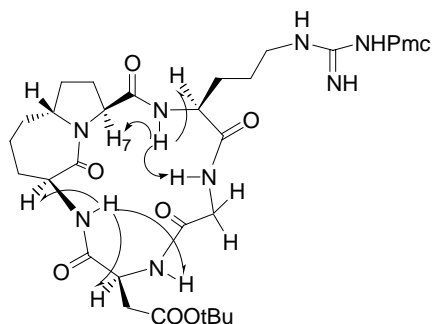


Figure 7. Key NOE connectivities found for mimetic **4a**.

In previous studies,³² we observed that the (5,7 *trans* 3*S*) lactam included in the pentapeptide **4a** is considered by modeling a very good β -turn inducer.

The ¹H NMR spectrum of **4a** in 3 mM CDCl₃ solutions exhibited amide protons in the range 7.19–7.94 ppm. These chemical shifts were characteristic of peptide backbone NHs strongly involved in hydrogen bonding. Since these hydrogen bonds cannot occur simultaneously, we propose that **4a** equilibrates between different folded conformations, similar to compound **3a**.

The middle- and long-range NOE cross-peaks observed in NOESY spectrum are summarized in Figure 7. A single conformation cannot account for all of these long-range NOEs; therefore, the NOESY data provide further evidence of multiple folded conformations. The NOE between Arg-NH and Gly-NH could arise from conformation SIV (Fig. 3). The NOE between Asp-NH and Lactam-NH is consistent with the γ -turn-like folding pattern SII (Fig. 3).

Compound **5a**, like compound **2a**, is more prone to aggregation so the spectra are recorded in 2 mM CDCl₃ solution. In this compound, the Arg residue is above the plane of the bicyclic lactam, while the *R* configuration of the stereocenter in position 3 orients the aspartic residue below the plane. So, Arg-NH cannot form a 10-membered ring hydrogen bonding with C=O(Asp). The chemical shift value of the amide protons Gly-NH (7.61 ppm) and Lactam-NH (7.49 ppm), and the temperature coefficients ($\Delta\delta\text{NH}/\Delta T = -4.2$ and -1.2 ppb/K, respectively) indicate that these protons are locked in an intramolecularly H-bonded state. Lactam-NH, inside to the cyclic pentapeptide, can form a γ -turn centered on aspartic residue. Protons Arg-NH and Asp-NH ($\delta\text{NH} = 6.99$ and 7.62 ppm, respectively; $\Delta\delta\text{NH}/\Delta T = -12.0$ ppb/K) are in equilibrium between a nonH-bonded and a H-bonded state. The NOESY spectrum shows the following cross-peaks: Asp-NH/Lactam-NH, Gly-NH/Arg-NH, Arg-NH/H6 (weak), Arg-NH/H7 and Arg-NH/Arg-H α strong (Fig. 8). These data provide further evidence for multiple folded conformations in equilibrium (type SII, SIII, and SIV geometries).

Amide proton–deuterium exchange rates provide information regarding the possible participation of an amide proton in a stable intramolecular H-bond within a sec-

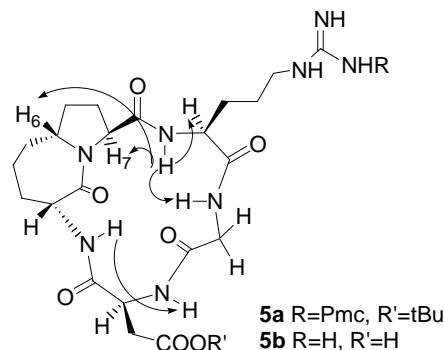


Figure 8. Key NOE connectivities found for mimetics **5a** and **5b**.

ondary or tertiary structural element (α -helix, β -sheet, and reverse turns). So, we analyzed the deprotected cyclopentapeptide mimics **1b–5b** (Fig. 2) in D₂O solution. In this solvent, the amide protons Arg-NH and Gly-NH of mimic **1b** exchange very slowly and this behavior suggests their involvement in strong intramolecular hydrogen bonds. The exchange is slow also for Lactam-NH of **2b** and **5b**, and for Arg-NH of compound **3b**.

After these results, we decided to study the conformational features of the most active compound **5b** in H₂O/D₂O (9:1) solution in order to observe the behavior of amide protons (Table 7). It is remarkable that the amide proton Gly-NH (7.65 ppm) is locked in an intramolecularly H-bonded state also in a competitive solvent like H₂O. The NOESY spectrum shows NOEs between Gly-NH and Arg-NH, and between Gly-NH and Arg-H α . These are indicative of a β -turn conformation stabilized by a hydrogen bond between Gly-NH and lactamic C=O. Moreover, the chemical shift and the slow exchange rate of Lactam-NH are indicative of a hydrogen-bonded proton that can form a γ -turn centered on aspartic residue. Protons Arg-NH and Asp-NH are solvent exposed; other significant NOE contacts are between Asp-NH/Lactam-NH, Asp-NH/Gly-H α_1 , and Asp-NH/Gly-H α_2 (Fig. 8). It is interesting to observe that the NOE contacts and the conformational preferences of compound **5b** are similar to those of analog pseudopeptide **5a**.

3. Discussion and conclusions

The crystal structure of the extracellular segment of integrin $\alpha_V\beta_3$ in complex with the cyclic pentapeptide ligand EMD121974 c(Arg-Gly-Asp-D-Phe-[NMe]Val) has been reported.³⁴ This structure provides the exact con-

Table 7. Chemical shifts (ppm) of NH protons of compounds **5a** in CDCl₃ and **5b** in H₂O/D₂O (9:1) solution

NH	5a ¹ H (CDCl ₃)	5b ¹ H (H ₂ O)	Down-field shift (ppm)
Arg	6.99	8.22	1.23
Gly	7.61	7.65	0.04
Asp	7.62	8.92	1.3
Lactam	7.49	7.95	0.54

formation of EMD121974 bound to $\alpha_V\beta_3$ integrin and can serve as a basis for understanding the general mode of interaction of integrins with other RGD-containing ligands.

Examination of the three-dimensional structure of the cyclic pentapeptide antagonist EMD121974 bound to the integrin $\alpha_V\beta_3$ (Protein Data Bank, entry 1L5G) reveals a conformation characterized by an inverse γ -turn with Asp at position ($i + 1$) and by a distorted β II'-turn with Gly and Asp at the ($i + 1$) and ($i + 2$) positions (Fig. 9). A distance between the C β atoms of Asp and Arg of 8.9 Å is observed in this pentapeptide bound conformation. Contrary to what had been assumed previously,²³ the inhibition of $\alpha_V\beta_3$ integrin does not require a strong kink of the RGD sequence. The type SIII geometry obtained by computational methods for the cyclopentapeptide mimics (see above, Fig. 3 and Table 4) is very similar to the X-ray binding conformation of EMD121974, in terms of backbone arrangement, intramolecular H-bonds, and C β –C β distance.

With the aim of identifying highly selective integrin antagonists, we synthesized and tested a small library of cyclic pseudopeptides in which the triad arginine, glycine, and aspartic acid (RGD) was attached to (5,6)- or (5,7)-fused bicyclic lactams with different configuration at two stereocenters. The use of rigid peptidomimetic scaffolds and conformationally constrained cyclic peptides that match biologically active conformation might enhance ligand binding for entropic reasons.

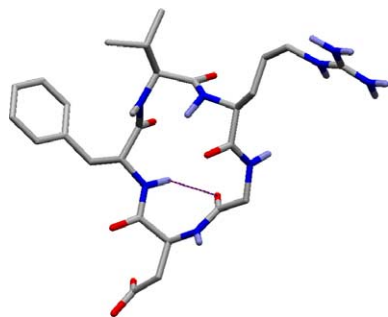


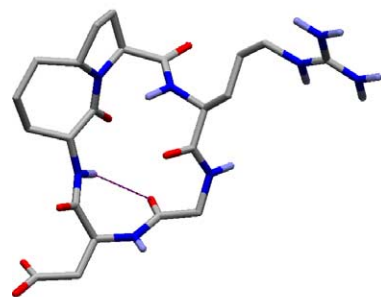
Figure 9. X-ray, $\alpha_V\beta_3$ -bound conformation of EMD121974 from 1L5G.³⁴

According to the results provided by spectroscopic and computational studies, a strong dependence of the cyclopeptide conformations on lactam ring size and stereochemistry has been observed. The effects of the structural constraint introduced by the bicyclic template on the conformation of the RGD sequence are mainly dictated by the turn mimetic properties of the scaffold.³²

Compounds **2b** and **5b**, containing the poor β -turn inducers bicyclic lactams 5,6 *trans* 3*R* and 5,7 *trans* 3*R*, respectively, show preferred cyclopeptide geometries featuring a lightly kinked or an almost extended conformation of the RGD sequence. Only type SIII (inverse γ -turn at Asp and distorted β II'-turn at Gly-Asp) and type SIV (β I-turn at Pro-Arg and inverse γ -turn at Asp) geometries can be detected among the conformers within 3 kcal/mol of the global minimum calculated for the simplified AGA cyclopeptide **2c** (Table 4). According to the H-bond analysis, these turns are populated by 40% (inverse γ -turn at Asp), 20% (distorted β II'-turn at Gly-Asp), and 26% (β I-turn at Pro-Arg) during the 10 ns MC/SD simulation of **2b** (Table 5). The average of the C β (Arg)–C β (Asp) distance is 8.8 Å over the same trajectory. The chemical shifts and the temperature dependence of amide protons Gly-NH and Lactam-NH of the protected cyclopeptide **2a** (Table 6), as well as NOE data (Fig. 5) and the slow exchange rate of Lactam-NH of **2b** in D₂O, provide evidence for the importance of the β -hairpin-like conformation of type SIV.

The lowest energy conformer of the simplified AGA cyclopeptide **5c** is characterized by an inverse γ -turn at Asp and by a distorted β II'-turn at Gly-Asp (type SIII geometry). Type SII and SIV geometries can be also detected among the conformers within 3 kcal/mol of the global minimum (Table 4). NMR data of compound **5a** provide evidence for different folded conformations in equilibrium, showing, in particular, the involvement of Lactam-NH in strong intramolecular hydrogen bonds (type SIII and SIV geometries). Compound **5b** in H₂O solution keeps the conformational preferences of the protected analog **5a**. Again Gly-NH and Lactam-NH are inner to the pentapeptide ring and one of the preferred conformations is stabilized by a β -turn and an inverse γ -turn (type SIV geometry). According to

A Type SIII



B Type SIV

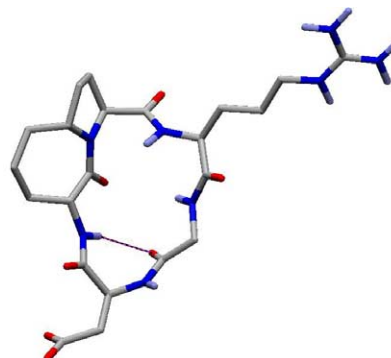


Figure 10. Conformations of **5b** sampled during the 10 ns MC/SD simulation after energy minimization. (A) Type SIII, inverse γ (Asp)/distorted β II' (Gly-Asp). (B) Type SIV, distorted β I (Pro-Arg)/inverse γ (Asp).

the H-bond analysis, the inverse γ -turn at Asp (33%) and the distorted β II'-turn at Gly-Asp (50%) and β I-turn at Pro-Arg (13%) are mainly populated during the 10 ns MC/SD simulation of **5b** (Table 5). The average of the C β (Arg)–C β (Asp) distance is 8.5 Å over the same trajectory. Remarkably, the 5,7 *trans* 3*R* bicyclic scaffold of compound **5b** appears to force the cyclopeptide to assume preferred conformations very similar to the X-ray $\alpha_v\beta_3$ -bound conformation of EMD121974. Energy-minimized conformations of **5b** obtained from frames featuring the binding requirements (type SIII geometry) or the SIV geometry and corresponding to the most populated geometries of the 10 ns MC/SD trajectory are shown in Figure 10. The root-mean-square (RMS) deviation in the rigid superimposition between the type SIII conformation of **5b** (Fig. 10A) and the X-ray structure of bound EMD121974 is 0.16 Å for the backbone atoms of the RGD sequence. Binding of **5b** might actually be enhanced by the high structural preorganization.

Compounds **2b** and **5b** showed the highest affinities to $\alpha_v\beta_3$ and inhibited radiolabeled echistatin binding to $\alpha_v\beta_3$ with an IC₅₀ of 14.3 ± 4.7 and 3.8 ± 0.9 nM, respectively. The conformational studies described above suggested that the type SIII and SIV geometries are the conformations mainly contributing to the conformational equilibria of cyclopeptides **2b** and **5b**. Both these geometries feature a minimal kink of the RGD sequence and an orientation of the Asp NH group suitable to maintain the same electrostatic and hydrogen bond ligand–receptor interactions observed in the crystalline complex of EMD121974 with $\alpha_v\beta_3$.

Conformational studies of compounds **1b**, **3b**, and **4b**, or related derivatives, containing efficient reverse-turn and β -turn inducer bicyclic lactams,³⁸ provide evidence for multiple folded conformations in equilibrium. In particular, the contribution of the SI structural type to these conformational equilibria is worth noting. This geometry features a strong kink of the RGD motif as a consequence of the β II'/ γ -turn arrangement with the bicyclic template in the *i* + 1 and *i* + 2 positions of the β II'-turn and the Gly residue in the *i* + 1 position of the γ -turn at the opposite side. According to the corresponding Arg-NH...O=C-Asp H-bond, the β II'-turn at bicyclic lactam is significantly populated during the MC/SD simulations of **1b**, **3b**, and **4b** (Table 5). The presence in conformational equilibria of geometries featuring kinked backbone conformations of the RGD sequence, short C β (Arg)–C β (Asp) distances, and inside orientation of the amide proton Asp-NH (γ -turn at Gly) might be responsible for reduced structural preorganization for binding and therefore for lower affinities to $\alpha_v\beta_3$ (Table 1).

Computational studies of **6b–7b** and **6c–7c** derivatives suggest that both the poor turn inducer bicyclic scaffolds 5,7 *cis* force the cyclopeptide to assume mainly the type SIII and SIV geometries. In spite of the proper orientation thus achieved by the pharmacophoric groups required for binding to the $\alpha_v\beta_3$ integrin, compounds **6b** and **7b** showed low affinities toward this receptor (Table

1). Docking studies⁴⁰ are currently in progress to gain deeper insights into ligand–receptor interactions of cyclic RGD pentapeptide mimics containing azabicycloalkane amino acids.

4. Materials and methods

4.1. Cell cultures

Primary cultures of bovine microvascular endothelial cells (BMECs) were obtained from bovine adrenal glands as described by Folkman.⁴¹ BMECs were maintained in DMEM supplemented with 20% fetal calf serum (FCS), 50 U/ml heparin (Sigma, St. Louis, MO), 50 μ g/ml bovine brain extract, and 100 U/ml gentamicin. Human umbilical vein endothelial cells (HUVECs) and human microvascular dermal endothelial cells (HMECs) were obtained from BioWhittaker (Walkersville, MD) and grown in EGM-2 (BioWhittaker).

4.2. Solid-phase receptor-binding assay

The receptor-binding assays were performed as described previously.^{42,43} Purified receptors $\alpha_v\beta_3$ and $\alpha_v\beta_5$ (Chemicon International Inc., Temecula, CA) were diluted, respectively, to 500 ng/ml and 1000 ng/well in coating buffer [20 mM Tris–HCl (pH 7.4), 150 mM NaCl, 2 mM CaCl₂, 1 mM MgCl₂, and 1 mM MnCl₂], whereas $\alpha_5\beta_1$ was diluted to 1000 ng/ml in 20 mM Tris–HCl (pH 7.4), 150 mM NaCl, and 1 mM MnCl₂. An aliquot of the diluted receptors (100 μ l/well) was added to 96-well microtiter plates and incubated overnight at 4 °C. The coating solution was removed by aspiration, and 200 μ l of blocking solution (coating buffer containing 1% bovine serum albumin (BSA)) was added to the wells, which were incubated for an additional 2 h at room temperature. After incubation, the plates were rinsed with 200 μ l of blocking solution (3 \times) and incubated with appropriate radiolabeled ligands for 3 h at room temperature. 0.05 and 0.1 nM [¹²⁵I]echistatin (Amersham Pharmacia) were used, respectively, for $\alpha_v\beta_3$ and $\alpha_v\beta_5$, whereas 20 nM [¹²⁵I]fibrinogen (Amersham Pharmacia) was used for $\alpha_5\beta_1$ receptor-binding assay. After incubation, the plates were sealed and counted in the γ -counter (Packard). Each data point is the result of the average of triplicate well, and was analyzed by nonlinear regression analysis with the Allfit program.

4.3. Platelet aggregation assay

Blood samples were collected in guinea pigs via cardiac puncture in 3.8% sodium citrate at a final dilution of 1–10. Platelet-rich plasma (PRP) was prepared by centrifugation at 120g for 10 min at room temperature. Platelet aggregation was assayed following the addition of TRAP 42-55 (Sigma), 25–100 μ M, to PRP at 37 °C by light transmission (4 channel aggregometer, PACKS-4, Helena Laboratories, Beaumont, Texas).

Vehicle or peptide solutions at different concentrations were added to aliquots of the same PRP, two minutes prior to TRAP addition. The extent of platelet aggrega-

tion was quantified as the maximum change in light transmission within 4 min after the addition of agonist.

The results were plotted (Allfit program) and expressed as the antagonist concentration that inhibited 50% of platelet aggregation.

4.4. Cell-adhesion assay

Ninety-six-well plates were coated with either fibronectin (Sigma, St. Louis, MO) or vitronectin (Calbiochem, San Diego, CA) (both at 5 µg/ml in phosphate-buffered saline) overnight at 4 °C. Approximately $4\text{--}5 \times 10^4$ cells/100 µl were seeded in each well and allowed to adhere for 1–3 h at 37 °C in the presence of various concentrations of RGD peptides. Nonadherent cells were removed with PBS and the remaining cells were fixed with 4% paraformaldehyde for 10 min. Adherent cells were stained with 1% toluidine blue for 10 min and rinsed with water. Stained cells were solubilized with 1% SDS and quantified on a microtiter plate reader at 600 nm (Victor², Wallac). Experiments were performed in quadruplicate and repeated at least three times. Results are expressed as mean compound concentration ± SEM that inhibited 50% of cell adhesion.

4.5. Computational studies

Conformational preferences of the RGD cyclopeptides have been investigated by molecular mechanics⁴⁴ calculations within the framework of MacroModel⁴⁵ version 5.5, using the MacroModel implementation of the Amber all-atom force field⁴⁶ (denoted AMBER*) and the implicit water GB/SA solvation model of Still et al.⁴⁷ A two-step protocol was used.

Monte Carlo/energy minimization (MC/EM) conformational searches⁴⁸ of the AGA (Ala-Gly-Ala) cyclopeptide analogs containing methyl groups instead of the Arg and Asp side chains were performed as the first step. The torsional space of each AGA cyclopeptide was randomly varied with the usage-directed Monte Carlo conformational search of Chang, Guida, and Still.⁴⁸ Ring-closure bonds were defined in the six- and seven-membered rings of the 5,6- and 5,7-fused bicyclic lactams, respectively, and in the cyclopeptide ring. Amide bonds were included among the rotatable bonds. For each search, at least 1000 starting structures for each variable torsion angle were generated and minimized until the gradient was less than 0.05 kJ/Åmol using the truncated Newton–Raphson method⁴⁹ implemented in MacroModel. Duplicate conformations and those with an energy greater than 6 kcal/mol above the global minimum were discarded. The nature of the stationary points individuated was tested by computing the eigenvalues of the second-derivative matrix.

Free simulations of the complete RGD cyclic peptides (Asp and Arg side chains were considered ionized) were then performed at 300 K using the metropolis Monte Carlo/stochastic dynamics (MC/SD) hybrid simulation algorithm,⁵⁰ starting from the cyclopeptide backbone geometries located by the previous MC/EM step.

RGD side-chain dihedral angles were defined as internal coordinate degrees of freedom in the Monte Carlo part of the algorithm. A time step of 1 fs was used for the stochastic dynamics (SD) part of the algorithm. At least two 10 ns simulations were run for each RGD cyclopeptide starting from different conformations to test the convergence. Samples were taken at 2 ps intervals during each simulation, yielding 5000 conformations for analysis.

4.6. NMR spectroscopy

All the spectra were acquired at a 400 MHz Bruker spectrometer equipped with pulsed field gradients. The following experiments were carried out (at 300 K): TOCSY, NOESY (mixing time 200, 400, and 600 ms), and HSQC.

The protected RGD-pentapeptides **1a–5a** (Fig. 2) were analyzed by NMR spectroscopy in CDCl₃ solution. We first performed ¹H NMR analysis to determine the lowest concentration at which intermolecular hydrogen bonding occurs.⁵¹ The data reported in this paper were obtained from samples at 300 K and 1–5 mM concentrations, at which aggregation was not significant. Traces of acid were removed from CDCl₃ by passing it through an alumina column. Amide hydrogen temperature coefficients were measured from 1D experiments carried out in the range 240–320 K. The cyclopentapeptide mimics **1b–5b** (Fig. 2) were analyzed by NMR spectroscopy in D₂O solution; compound **5b** was also studied in H₂O/D₂O (9:1) solution.

Acknowledgments

The authors thank CNR and MIUR (COFIN and FIRB research programs) for financial support and CILEA for computing facilities.

Supplementary data

Description of the synthesis and experimental data for the preparation of compound **5b**. Tables S1–S6 listing the ¹H and ¹³C NMR chemical shifts δ (ppm) of pseudo-pentapeptides **1a–7a** and **1b–7b**. Supplementary data associated with this article can be found in the online version at doi:10.1016/j.bmc.2005.08.048.

References and notes

1. Gumbiner, B. M. *Cell* **1996**, *84*, 345.
2. Aplin, A. E.; Howe, A.; Alahari, S. K.; Juliano, R. L. *Pharmacol. Rev.* **1998**, *50*, 197.
3. Eliceiri, B. P.; Cheresch, D. A. *Curr. Opin. Cell Biol.* **2001**, *13*, 563.
4. Hood, J. D.; Cheresch, D. A. *Nat. Rev. Cancer* **2002**, *2*, 91.
5. Howe, A.; Aplin, A. E.; Alahari, S. K.; Juliano, R. L. *Curr. Opin. Cell Biol.* **1998**, *10*, 220.
6. Hynes, R. O. *Cell* **2002**, *110*, 673.
7. Hynes, R. O. *Cell* **1987**, *48*, 549.
8. Giancotti, F. G.; Ruoslahti, E. *Science* **1999**, *285*, 1028.

9. Ruoslahti, E.; Pierschbacher, M. D. *Science* **1987**, *238*, 491.
10. Ruoslahti, E. *Ann. Rev. Cell Dev. Biol.* **1996**, *12*, 697.
11. Plow, E. F.; Haas, T. A.; Zhang, L.; Loftus, J.; Smith, J. W. *J. Biol. Chem.* **2000**, *275*, 21785.
12. Suehiro, K.; Smith, J. W.; Plow, E. F. *J. Biol. Chem.* **1996**, *271*, 10365.
13. Eliceiri, B. P.; Cheresh, D. A. *J. Clin. Invest.* **1999**, *103*, 1227.
14. Brooks, P. C.; Clark, R. A. F.; Cheresh, D. A. *Science* **1994**, *264*, 569.
15. Brooks, P. C.; Stromblad, S.; Klemke, R.; Visscher, D.; Sarkar, F. H.; Cheresh, D. A. *J. Clin. Invest.* **1995**, *96*, 1815.
16. Kumar, C. C.; Malkowski, M.; Yin, Z.; Tanghetti, E.; Yaremko, B.; Nechuta, T.; Varner, J.; Liu, M.; Smith, E. M.; Neustadt, B.; Presta, M.; Armstrong, L. *Cancer Res.* **2001**, *61*, 2232.
17. Friedlander, M.; Brooks, P. C.; Shaffer, R. W.; Kincaid, C. M.; Varner, J. A.; Cheresh, D. A. *Science* **1995**, *270*, 1500.
18. Mitjans, F.; Meyer, T.; Fittschen, C.; Goodman, S.; Jonczyk, A.; Marshall, J. F.; Reyes, G.; Piulats, J. *Int. J. Cancer* **2000**, *87*, 716.
19. MacDonald, T. J.; Taga, T.; Shimada, H.; Tabrizi, P.; Zlokovic, B. V.; Cheresh, D. A.; Laug, W. E. *Neurosurgery* **2001**, *48*, 151.
20. Scarborough, R. M.; Naughton, M. A.; Teng, W. E.; Rose, J. W.; Phillips, D. R.; Nannizzi, L.; Arfsten, A.; Campbell, A. M.; Charo, I. F. *J. Biol. Chem.* **1993**, *268*, 1066.
21. Bach, A. C., II; Espina, J. R.; Jackson, S. A.; Stouten, P. F. W.; Duke, J. L.; Mousa, S. A.; DeGrado, W. F. *J. Am. Chem. Soc.* **1996**, *118*, 293.
22. Müller, G.; Gurrath, M.; Kessler, H. *J. Comput.-Aided Mol. Des.* **1994**, *8*, 709.
23. Haubner, R.; Gratiar, R.; Diefenbach, B.; Goodman, S. L.; Jonczyk, A.; Kessler, H. *J. Am. Chem. Soc.* **1996**, *118*, 7461.
24. Haubner, R.; Finsinger, D.; Kessler, H. *Angew. Chem. Int. Ed. Engl.* **1997**, *36*, 1374.
25. Wermuth, J.; Goodman, S. L.; Jonczyk, A.; Kessler, H. *J. Am. Chem. Soc.* **1997**, *119*, 1328.
26. Lohof, E.; Planker, E.; Mang, C.; Burkhart, F.; Dechantsreiter, M. A.; Haubner, R.; Wester, H.-J.; Schwaiger, M.; Hölzemann, G.; Goodman, S. L.; Kessler, H. *Angew. Chem. Int. Ed. Engl.* **2000**, *39*, 2761.
27. Schumann, F.; Müller, A.; Koks, M.; Müller, G.; Sewald, N. *J. Am. Chem. Soc.* **2000**, *122*, 12009.
28. Haubner, R.; Schmitt, W.; Hölzemann, G.; Goodman, S. L.; Jonczyk, A.; Kessler, H. *J. Am. Chem. Soc.* **1996**, *118*, 7881.
29. Dechantsreiter, M. A.; Planker, E.; Mathä, B.; Lohof, E.; Hölzemann, G.; Jonczyk, A.; Goodman, S. L.; Kessler, H. *J. Med. Chem.* **1999**, *42*, 3033.
30. Belvisi, L.; Bernardi, A.; Checchia, A.; Manzoni, L.; Potenza, D.; Scolastico, C.; Castorina, M.; Cupelli, A.; Giannini, G.; Carminati, P.; Pisano, C. *Org. Lett.* **2001**, *3*, 1001.
31. Angiolini, M.; Araneo, S.; Belvisi, L.; Cesarotti, E.; Checchia, A.; Crippa, L.; Manzoni, L.; Scolastico, C. *Eur. J. Org. Chem.* **2000**, 2571.
32. Belvisi, L.; Bernardi, A.; Manzoni, L.; Potenza, D.; Scolastico, C. *Eur. J. Org. Chem.* **2000**, 2563.
33. The bicyclic lactams incorporate a natural C α (S) proline residue, but vary in the lactam ring size (6 or 7), and in the stereochemistry at the bridgehead and at the N-bearing carbon C3. They are classified according to the C3 configuration as (3*S*) or (3*R*) bicycles. For convenience, to indicate the bridgehead configuration, the *cis* and *trans* descriptors are used, depending on the relative position of the hydrogen atoms at the bridgehead and the Pro C α carbon.
34. Xiong, J.-P.; Stehle, T.; Zhang, R.; Joachimiak, A.; Frech, M.; Goodman, S. L.; Arnout, M. A. *Science* **2002**, *296*, 151.
35. The use of [¹²⁵I]echistatin as radiolabeled ligand in integrin receptor-binding assays toward $\alpha_v\beta_3$ and $\alpha_v\beta_5$ has been reported in previous literature Ref. 16,42 showing data consistent with our results. However, binding data and selectivity may differ significantly when alternate ligand and/or binding assay is used. For example, EMD121974 is reported to be 10-fold more selective for $\alpha_v\beta_3$ in binding assay using vitronectin as the ligand.⁵²
36. The large-scale synthetic approach to **5b** is reported in the supporting material.
37. Rose, G. D.; Gierasch, L. M.; Smith, J. A. *Adv. Prot. Chem.* **1985**, *37*, 1–109.
38. Previous computational studies³² suggested the following trend in β -turn inducing properties of bicyclic lactams: 5,6 *trans* *S* > 5,7 *trans* *S* > 5,6 *cis* *S*.
39. In solvent such as CDCl₃, NH amide protons that are involved in hydrogen bonding resonate around δ 6.5–8 ppm.
40. Docking studies of selected peptidic, pseudopeptidic, and nonpeptidic ligands into the $\alpha_v\beta_3$ and $\alpha_v\beta_5$ integrin binding sites have been recently reported. (a) Marinelli, L.; Lavecchia, A.; Gottschalk, K.-E.; Novellino, E.; Kessler, H. *J. Med. Chem.* **2003**, *46*, 4393; (b) Marinelli, L.; Gottschalk, K.-E.; Meyer, A.; Novellino, E.; Kessler, H. *J. Med. Chem.* **2004**, *47*, 4166; (c) Moitessier, N.; Henry, C.; Maigret, B.; Chapleur, Y. *J. Med. Chem.* **2004**, *47*, 4178.
41. Folkman, J.; Haudenschild, C. C.; Zetter, B. R. *Proc. Natl. Acad. Sci. U.S.A.* **1979**, *76*, 5217.
42. Kumar, C. C.; Nie, H.; Rogers, C. P.; Malkowski, M.; Maxwell, E.; Catino, J. J.; Armstrong, L. *J. Pharmacol. Exp. Ther.* **1997**, *283*, 843.
43. Suehiro, K.; Gailit, J.; Plow, E. F. *J. Biol. Chem.* **1997**, *272*, 5360.
44. Burkert U.; Allinger N. L. *Molecular Mechanics*. ACS Monograph 177, American Chemical Society, Washington, DC, 1982.
45. Mohamadi, F.; Richards, N. G. J.; Guida, W. C.; Liskamp, R.; Lipton, M.; Caufield, C.; Chang, G.; Hendrickson, T.; Still, W. C. *J. Comput. Chem.* **1990**, *11*, 440.
46. Weiner, S. J.; Kollman, P. A.; Nguyen, D. T.; Case, D. A. *J. Comput. Chem.* **1986**, *7*, 230.
47. Still, W. C.; Tempczyk, A.; Hawley, R. C.; Hendrickson, T. *J. Am. Chem. Soc.* **1990**, *112*, 6127.
48. Chang, G.; Guida, W. C.; Still, W. C. *J. Am. Chem. Soc.* **1989**, *111*, 4379.
49. Ponder, J. W.; Richards, F. M. *J. Comput. Chem.* **1987**, *8*, 1016.
50. Guarnieri, F.; Still, W. C. *J. Comput. Chem.* **1994**, *15*, 1302.
51. Gardner, R. R.; Liang, G.-B.; Gellman, S. H. *J. Am. Chem. Soc.* **1999**, *121*, 1806.
52. Goodman, S. L.; Hölzemann, G.; Sulyok, G. A. G.; Kessler, H. *J. Med. Chem.* **2002**, *45*, 1045.